01 Jan 1993

Efficient Simulation Of Multicarrier Digital Communication Systems In Nonlinear Channel Environments

Kevin W. Schneider

William H. Tranter
Missouri University of Science and Technology

Recommended Citation

K. W. Schneider and W. H. Tranter, "Efficient Simulation Of Multicarrier Digital Communication Systems In Nonlinear Channel Environments," *IEEE Journal on Selected Areas in Communications*, vol. 11, no. 3, pp. 328 - 339, Institute of Electrical and Electronics Engineers, Jan 1993.
The definitive version is available at https://doi.org/10.1109/49.219548

Efficient Simulation of Multicarrier Digital Communication Systems in Nonlinear Channel Environments

Kevin W. Schneider, *Member, IEEE,* and William H. Tranter, *Fellow, IEEE*

***Abstract*—The effectiveness of computer simulation as a tool for the design and analysis of communication systems is often limited by the long execution times required for many simulations. When simulating multicarrier digital communication systems operating over nonlinear channels, the required high sampling rate contributes significantly to long execution times. A new method that reduces the sampling rate of simulations of such systems is developed. This Partial Sum of Products (ParSOP) method reduces the sampling rate by generating only the intermodulation products that lie in a frequency band of interest. The ParSOP method requires that the bandpass nonlinearity be represented by memoryless operations on the complex envelope of the signal and that the subcarriers constituting the frequency-division multiplexed signal are sufficiently separated to prevent significant adjacent channel interference. Simulation results for such systems show that an order of magnitude reduction in the sampling rate is possible while producing only minimal error in the bit error rate estimate.**

I. Introduction

OVER the past few years, computer simulation has become an important tool for both the analysis and design of complex communication systems [1], [2]. The use of simulation is often limited, however, by the long run times that are necessary for the determination of the system performance, especially the bit error rate (BER). This problem becomes more acute if the transmitted signal contains a multiplex of channels, generated by frequency-division multiplexing, because the large resulting bandwidth necessitates a high sampling frequency in the simulation. If, in addition, the channel contains nonlinear elements, intermodulation distortion further increases the bandwidth of the signals present in the system. These effects demand an even higher sampling frequency which leads to simulation run times that are proportionately longer.

When simulating a system that uses frequency-division multiplexing (FDM), one usually concentrates on a single channel within the system for conducting a performance analysis. Using lowpass decomposition, the center frequency of the bandpass channel of interest is usually translated to zero frequency. The other channels in the FDM signal are only important if they give rise to distortion in the channel of interest. If the channel spacing is sufficiently wide, and if the system is linear, these other channels can usually be neglected and therefore need not be included in the simulation. If the channel is nonlinear, however, intermodulation distortion results in significant energy from the channels other than the channel of interest being folded into the channel of interest. In this case, obviously, these other channels must be included in the simulation since they give rise to errors in the channel of interest.

When the subcarriers that comprise the FDM signal have constant envelopes and the number of subcarriers is large, the intermodulation distortion is often modeled by an additive Gaussian noise source [3]. Using this model, one of a variety of techniques can be employed to find the noise power spectral density [4]–[6] or the power contained in a particular intermodulation product [7]. Unfortunately, these techniques are not applicable when the subcarriers do not have constant envelopes, since the intermodulation products will be correlated with the signal of interest and with each other [8]. This case of nonconstant envelope subcarriers arises often when working with digital communication systems operating over bandlimited channels. For such systems, the effect of the intermodulation distortion can only be determined by simulating the interaction between the subcarriers that produces the intermodulation distortion. Unfortunately, because of the multiplexing and the nonlinearity, the resulting simulation will require an extremely high sampling rate, and a correspondingly long execution time.

In order to reduce the sampling rate for simulations of FDM digital communication systems where the multiplexed signal passes through a nonlinear device, we present a new simulation method called the Partial Sum of Products (ParSOP) method. The ParSOP method involves the decomposition of the signal at the output of the nonlinear device into a sum of products. Each product is composed of baseband versions of the individual modulated subcarriers that constitute the undistorted FDM signal. The "partial" portion of the sum includes only those products that have significant energy within the bandwidth of the single subcarrier of interest. If the channel spacing is sufficiently wide, the partial sum will include only those products that are centered in the channel of interest. The resulting reduction in the simulation bandwidth is shown in Fig. 1. With the ParSOP method, the simulation sampling

Manuscript received March 5, 1992; revised September 8, 1992. This paper was presented in part at the 1992 IEEE Military Communications Conference, San Diego, CA, Oct. 11–14, 1992.

K. W. Schneider is with ADTRAN, Inc., 901 Explorer Blvd., Huntsville, AL 35806-2807.

W. H. Tranter is with the Department of Electrical Engineering, University of Missouri–Rolla, Rolla, MO 65401.

IEEE Log Number 9207823.

0733–8716/93$03.00 © 1993 IEEE

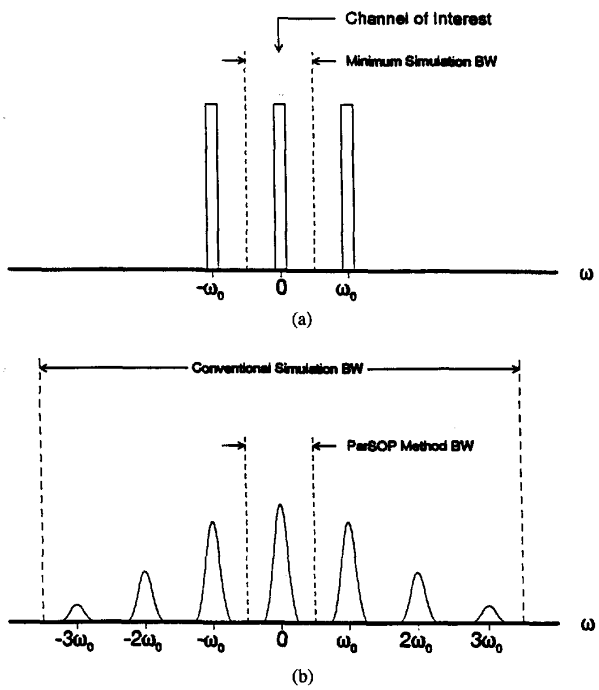

Fig. 1. (a) Spectrum of a sample three-channel FDM signal. (b) Spectrum of third-order intermodulation products.

rate need only be sufficiently large to accurately model the intermodulation products falling within the channel of interest rather than having to be large enough to simulate the entire system bandwidth. It will be demonstrated that the ParSOP method can produce significant savings in the simulation run time.

II. System Model

The digital communication system being considered is modeled as shown in Fig. 2. In this model, a frequency-division multiplexed (FDM) signal is the input to a bandpass nonlinear device. The nonlinear device is modeled by a cascade of a zonal bandpass filter, a nonlinearity, and a second zonal bandpass filter. The zonal filter is assumed to pass the fundamental component of the signal, centered around ω_c (the input carrier frequency), without distortion while rejecting all other harmonics of the signal [9]. This filter is necessary in the simulation model since all signals in the simulation must be bandlimited to ensure that they may be sampled without aliasing. The nonlinearity may or may not contain memory, but it is assumed that a frequency-independent describing function [10] or complex envelope characteristic [11] is sufficient to represent the bandpass device. The nonlinear device is assumed to be followed by an additive Gaussian noise source. After the addition of noise, the signals are demultiplexed, and each modulated subcarrier is fed to its respective demodulator and data detector. As mentioned in the Introduction, it is usually desirable to demodulate and observe only one subcarrier in a given simulation. We will refer to this observed subcarrier as the kth subcarrier.

A mathematical model of the assumed communication system is shown in Fig. 3. In this model, the signal $x(t)$, a frequency-division multiplexed signal consisting of N modulated subcarriers, is the input to the nonlinear device. This composite signal can be written in the form

$$x(t) = \sum_{i=1}^{N} s_i(t) \cos\left[(\omega_c + \omega_i)t + \phi_i(t)\right] \tag{1}$$

where ω_c is the channel carrier frequency, $s_i(t)$ is the ith subcarrier envelope, ω_i is the ith subcarrier frequency, and $\phi_i(t)$ is the ith subcarrier phase. Both the envelope and the phase of each subcarrier may be affected by the data modulation. The complex envelope of $x(t)$ can be written as

$$\tilde{x}(t) = \sum_{i=1}^{N} \tilde{s}_i(t) e^{j\omega_i t} \tag{2}$$

where

$$\tilde{s}_i(t) = s_i(t) e^{j\phi_i(t)} \tag{3}$$

is the complex envelope of the ith subcarrier. The complex envelope of the signal $x(t)$ can also be written

$$\tilde{x}(t) = V(t) e^{j\theta(t)} \tag{4}$$

where the envelope, $V(t)$, of the composite signal, $x(t)$, is the positive square root of the expression

$$[V(t)]^2 = \tilde{x}(t)\tilde{x}^*(t) = \sum_{i=1}^{N}\sum_{j=1}^{N} \tilde{s}_i(t)\tilde{s}_j^*(t) e^{j(\omega_i - \omega_j)t}. \tag{5}$$

The phase $\theta(t)$ is given by

$$\theta(t) = \tan^{-1}\left(\frac{\sum_{i=1}^{N} \sin\left[\omega_i t + \phi_i(t)\right]}{\sum_{i=1}^{N} \cos\left[\omega_i t + \phi_i(t)\right]}\right). \tag{6}$$

A bandpass nonlinear device (such as a traveling-wave-tube amplifier) is typically characterized by two functions, referred to as the amplitude-modulation-to-amplitude-modulation (AM/AM) and amplitude-modulation-to-phase-modulation (AM/PM) conversion characteristics [11]. For our purposes, however, it is more convenient to characterize the bandpass nonlinear device by a complex function, $\boldsymbol{h}[V]$, that can be obtained from the AM/AM and AM/PM characteristics. The complex envelope of the output of the bandpass nonlinear device, $\tilde{z}_{\text{Out}}(t)$, is then given by

$$\tilde{z}_{\text{Out}}(t) = \boldsymbol{h}[V(t)] e^{j\theta(t)} \tag{7}$$

where $V(t)$ is the signal envelope at the input to the nonlinearity. Various forms for the nonlinear characteristic $\boldsymbol{h}[V]$ have been used to model amplifiers found in satellite communication systems [4], [12], [13]. Of these, a complex power series model lends itself well to a direct derivation of the ParSOP method. When using the power series model, the nonlinear characteristic is represented by a complex power series that includes only odd-order terms. (The relationship between this

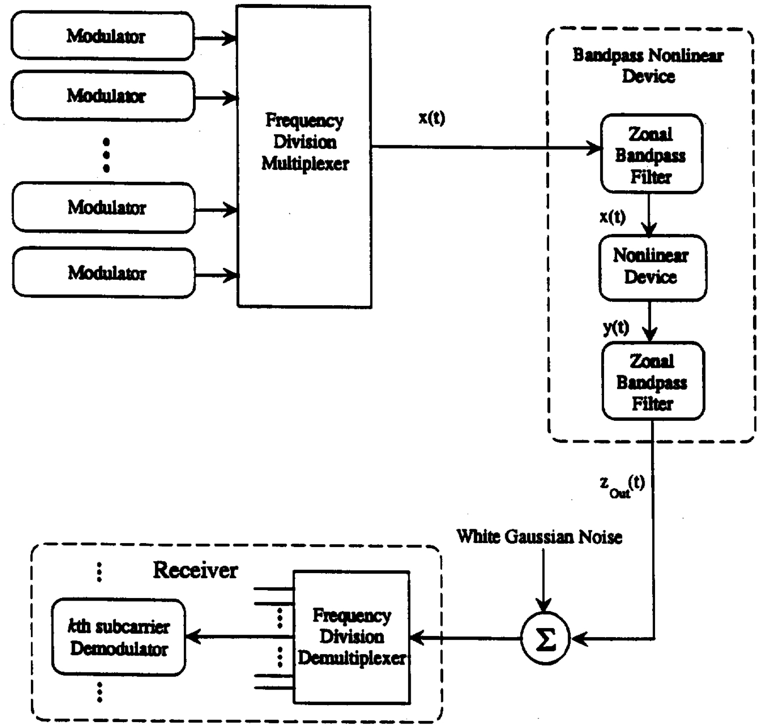

Fig. 2. Block diagram of the digital communication system model.

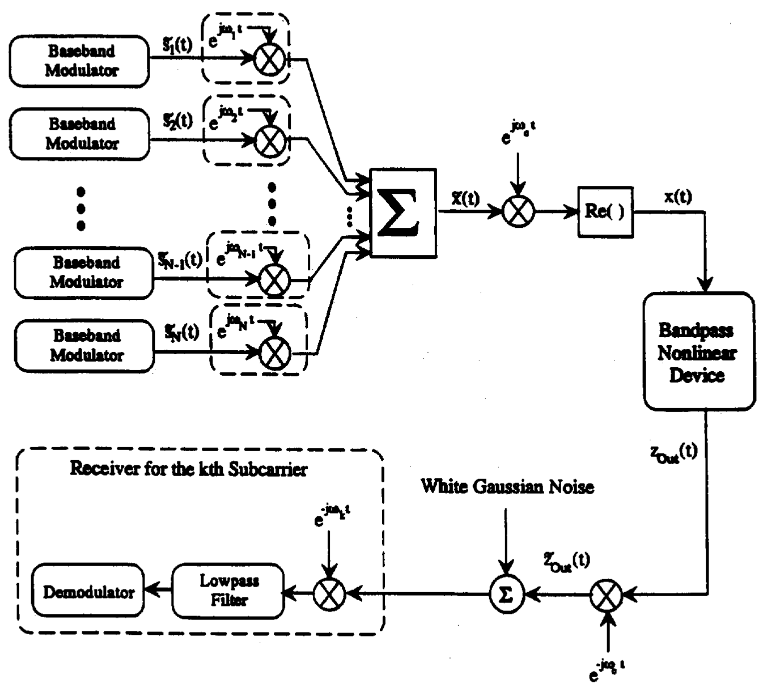

Fig. 3. Block diagram of the mathematical model of the FDM digital communication system.

envelope model and an instantaneous model can be found in [8]. A more comprehensive treatment of the subject can be found in [14].) In any practical implementation of this model, the series must be truncated to a finite number of terms. The result is a complex polynomial of degree $2R+1$, where the value of R is selected as a tradeoff between model complexity and model accuracy. This polynomial model is written in equation form as

$$\boldsymbol{h}[V(t)] = \sum_{r=0}^{R} C_r V(t)^{2r+1}. \tag{8}$$

Other forms for the nonlinear device characteristic can be used with the ParSOP method by using the derivation presented in Section III-B.

III. Derivation of the ParSOP Method

Having defined the system to be investigated, we now consider the derivation of the ParSOP method. This is accomplished using two different methods. First, the ParSOP method is derived directly in the time-domain using the truncated power series model of the nonlinear device. We then outline an alternative derivation of the ParSOP method that allows more flexibility in the characterization of the nonlinear model but is less straightforward than the direct derivation.

A. Direct Derivation of the ParSOP Method

When the nonlinear device in the communication system is modeled by a truncated power series, the ParSOP method can be derived directly. This direct derivation is accomplished by writing the output signal in terms of a sum of products composed of only the complex envelopes of the modulated subcarriers. This derivation of the ParSOP method requires that the nonlinear device output can be obtained in the form of a sum of products (SOP). Once the SOP is obtained, the selection of products to be retained in the partial sum can be made.

As an initial step toward the formation of the SOP, we wish to express the output of the nonlinear device in terms of the modulated subcarriers. The first step toward accomplishing this goal is to use (7) and (8) to obtain

$$\begin{aligned}\tilde{z}_{\text{Out}}(t) &= \boldsymbol{h}[V(t)]e^{j\theta(t)} \\ &= \left[\sum_{r=0}^{R} C_r [V(t)]^{2r}\right] V(t)e^{j\theta(t)} \\ &= \left[\sum_{r=0}^{R} C_r [V(t)]^{2r}\right] \tilde{x}(t).\end{aligned} \tag{9}$$

The next step is to substitute (5) for $[V(t)]^2$ and (2) for $\tilde{x}(t)$ in (9). This results in

$$\tilde{z}_{\text{Out}}(t) = \sum_{r=0}^{R} C_r D_r \tag{10}$$

where

$$D_r = \left[\sum_{i=1}^{N}\sum_{j=1}^{N} \tilde{s}_i(t)\tilde{s}_j^*(t)e^{j(\omega_i-\omega_j)t}\right]^r \left[\sum_{m=1}^{N} \tilde{s}_m(t)e^{j\omega_m t}\right]. \tag{11}$$

The substitution for $[V(t)]^2$ in terms of the input subcarriers is a direct consequence of using a power series expansion for $\boldsymbol{h}[V]$ containing only odd powers of the input envelope.

We next expand the expression for D_r, using i with an odd subscript to replace each of the r occurrences of the index i, and i with an even number subscript to replace each of the r occurrences of the index j. This yields

$$\begin{aligned}D_r = \sum_{m=1}^{N}\sum_{i_1=1}^{N}\sum_{i_2=1}^{N}\cdots\sum_{i_{2r-1}=1}^{N}\sum_{i_{2r}=1}^{N} &\tilde{s}_m(t)\tilde{s}_{i_1}(t)\tilde{s}_{i_2}^*(t)\cdots \\ &\tilde{s}_{i_{2r-1}}(t)\tilde{s}_{i_{2r}}^*(t)e^{j(\omega_m+\omega_{i_1}-\omega_{i_2}+\cdots+\omega_{i_{2r-1}}-\omega_{i_{2r}})t}\end{aligned} \tag{12}$$

Substituting this expression for D_r into (10), we have the complex envelope of the output written as a sum of products. The result is

$$\begin{aligned}\tilde{z}_{\text{Out}}(t) = &\sum_{r=0}^{R}\sum_{m=1}^{N}\sum_{i_1=1}^{N}\sum_{i_2=1}^{N}\cdots\sum_{i_{2r-1}=1}^{N}\sum_{i_{2r}=1}^{N} \\ &\cdot C_r\tilde{s}_m(t)\tilde{s}_{i_1}(t)\tilde{s}_{i_2}^*(t)\cdots\tilde{s}_{i_{2r-1}}(t)\tilde{s}_{i_{2r}}^*(t)e^{j\omega_d t}\end{aligned} \tag{13}$$

where

$$\omega_d = \omega_k + (\omega_{i_1} - \omega_{i_2}) + \cdots + (\omega_{i_{2r-1}} - \omega_{i_{2r}}). \tag{14}$$

Each term in the sum represents a unique intermodulation product (IMP). The $r = 0$ term is the undistorted input signal passed through the nonlinearity to the output. The other terms in the sum represent the intermodulation distortion (IMD).

To realize the reduction in simulation runtime that is possible with the ParSOP method, we approximate (13) by a partial sum that includes only those IMP's that have significant energy within the bandwidth of the subcarrier of interest (the kth subcarrier). For most nonlinearities, the IMP's of interest will be those centered in or near the channel of interest. If we are observing the kth subcarrier, we only retain the IMP's that are centered at ω_k. These are the IMP's for which $\omega_d = \omega_k$. The approximation to the output signal for the frequencies near ω_k is called $\tilde{z}_{\text{Out},\omega_k}(t)$, and it is given by

$$\begin{aligned}\tilde{z}_{\text{Out}\omega_k}(t) = &\sum_{r=0}^{R}\sum_{m=1}^{N}\sum_{i_1=1}^{N}\sum_{i_2=1}^{n}\cdots\sum_{i_{2r-1}=1}^{N}\sum_{i_{2r}=1}^{N} \\ &\cdot C_r\tilde{s}_m(t)\tilde{s}_{i_1}(t)\tilde{s}_{i_2}^*(t)\cdots\tilde{s}_{i_{2r-1}}(t)\tilde{s}_{i_{2r}}^*(t)e^{j\omega_d t} \\ &\cdot \boldsymbol{H}[\omega_d, \omega_k]\end{aligned} \tag{15}$$

where ω_d is given by (14) and $\boldsymbol{H}[\omega_d, \omega_k]$ is an indicator function defined by

$$\boldsymbol{H}[\omega_d, \omega_k] = \begin{cases} 1, & \omega_d = \omega_k \\ 0, & \text{otherwise} \end{cases} \tag{16}$$

which specifies which terms of the sum are to be included in the partial sum.

By examining (15), we can see the benefits that the ParSOP method brings to simulation. First, the IMP's can be found as the product of lowpass signals. Specifically, these signals are the complex envelopes of the modulated subcarriers. If we choose ω_c so that $\omega_k = 0$ (which can be done without loss of generality), then the sum of the nonzero IMP's in (15) is also a lowpass signal. Since (15) consists of only terms that are centered at zero frequency, its sampling frequency can be much lower than that of (13). This reduction in the sampling rate is what makes the ParSOP method attractive as a simulation tool.

B. An Alternative Derivation of the ParSOP Method

Although the direct derivation of the ParSOP method is only applicable when the nonlinear device characteristic can be represented by a complex power series, the ParSOP method can be used with other nonlinear models by utilizing the work of Shimbo [4] and Fuenzalida *et al.* [12]. In this subsection, we describe their work and outline a derivation of the ParSOP method which makes use of their results. This derivation encompasses a broader class of systems than the previous direct derivation, since it only requires that the nonlinear device can be modeled as a bandpass memoryless nonlinearity. To relate this derivation to the preceding direct derivation, the specific case of the power series model is briefly considered.

The work of Fuenzalida *et al.* [12] was directed toward finding the output of a bandpass nonlinear device, given an FDM signal on the input. From their results, assuming that the nonlinear device is characterized by (7) and the FDM input signal is given by (1), the complex envelope of the nonlinear device output is given by

$$\tilde{z}_{\mathrm{Out}}(t) = \sum_{\substack{k_1,k_2,\cdots,k_N=-\infty \\ (k_1+k_2+\cdots k_N=1)}}^{\infty} \cdot \left[\exp\left(j\sum_{i=1}^{N} k_i[\omega_i t + \phi_i(t)]\right)\boldsymbol{M}(k_1,k_2,\cdots,k_N;t)\right]. \tag{17}$$

The function $\boldsymbol{M}(k_1,k_2,\cdots,k_n;t)$, which first appeared in [4], will be referred to as the Shimbo Amplitude Function (SAF) and will be defined later. The condition $\Sigma_{i=1}^{N} k_i = 1$ restricts the sum to only those terms that lie in the zone of the first harmonic (the fundamental) of the output of a wideband nonlinear device. To see why this condition has the desired effect, we must remember that we are using the complex envelope notation for the signals in this equation. The complex envelope notation masks the carrier component that is present in each term of the exponential sum. The weighted sum of these carriers must equal the original carrier frequency, ω_c, for the terms to lie in the zone of the first harmonic of the output signal. This requirement can be expressed mathematically as

$$\exp\left(j\sum_{i=1}^{N} k_i\omega_c t\right) = e^{j\omega_c t} \tag{18}$$

which can be reduced to the condition $\Sigma_{i=1}^{N} k_i = 1$ included in (17). As a result, the terms in (17) are the terms of the sum that lie in the zone about the fundamental carrier frequency.

The SAF, $\boldsymbol{M}(k_1,k_2,\cdots,k_N;t)$ in (17), can be expressed as [12]

$$\boldsymbol{M}(k_1,k_2,\cdots,k_N;t) = \int_0^{\infty} r\left\{\prod_{i=1}^{N} J_{k_i}[V_i(t)r]\right\}\int_0^{\infty}\rho\boldsymbol{h}(\rho)J_1(r\rho)\,d\rho\,dr \tag{19}$$

where $J_i(x)$ denotes the ith-order Bessel function of the first kind, and $\boldsymbol{h}(x)$ is the nonlinear characteristic. The derivation of this expression involves the use of the Fourier transform of the nonlinear characteristic and the use of a Bessel series expansion for the resulting complex exponential. The variables of integration, ρ and r, result from the double Fourier transform of the complex characteristic of the nonlinear device. (Since we are using lowpass representations of bandpass signals, the signal on the input of the nonlinear characteristic is complex, and a double Fourier transform must be taken over the real and imaginary input amplitude levels.) If the nonlinear device does not exhibit any AM/PM conversion, the SAF will be real, but in general it is complex, representing both envelope distortion and a variable phase shift. However, its value depends only on the envelopes of the input subcarriers and not their phases.

As noted in the previous section, the ParSOP method gains its computational advantage by generating only those intermodulation products that lie in the bandwidth of interest. These are the products for which

$$\sum_{i=1}^{N} k_i\omega_i = \omega_k. \tag{20}$$

The resulting expression for the ParSOP approximation to the output of the nonlinearity within the bandwidth of the kth subcarrier is

$$\tilde{z}_{\mathrm{Out},\omega_k}(t) = \sum_{\substack{k_1,k_2,\cdots k_N=-\infty \\ (k_1+k_2+\cdots+k_N=1) \\ (k_1\omega_1+k_2\omega_2+\cdots+k_n\omega_N=\omega_k)}}^{\infty} \cdot \left[\exp\left(j\sum_{i=1}^{N} k_i[\omega_i t + \theta_i(t)]\right)\boldsymbol{M}(k_1,k_2,\cdots,k_N;t)\right]. \tag{21}$$

To use this formula, the SAF must be evaluated specifically for each type of nonlinearity. This is addressed Appendix A.

IV. Use of ParSOP in Analysis

The bit error rate of digital communication systems that contain nonlinear elements cannot typically be evaluated only through theoretical analysis. However, by employing the ParSOP method, an analytical estimate of the bit error rate by can be obtained for some systems, an example of which is shown in Fig. 4. When the ParSOP method is used in this way, it is referred to as the Analytic ParSOP Method.

Fig. 4 shows a three subcarrier system having the three complex envelope signals: $\tilde{s}_1(t), \tilde{s}_2(t)$, and $\tilde{s}_3(t)$. The subcarrier of interest is assumed to be $\tilde{s}_1(t)$, which is located in the subchannel in which we are conducting the performance analysis. The signals $\tilde{s}_2(t)$ and $\tilde{s}_3(t)$ represent subcarriers that are located at frequencies ω_D above and below the center frequency of $\tilde{s}_1(t)$. In this system, the complex envelope of the signal at the input to a band-pass nonlinear device is given by

$$\tilde{x}(t) = \tilde{s}_1(t) + \tilde{s}_2(t)e^{j\omega_D t} + \tilde{s}_3(t)e^{-j\omega_D t}. \tag{22}$$

We will assume a third-order nonlinearity defined by the bandpass characteristic

$$\boldsymbol{h}[V(t)] = C_0V(t) + C_1[V(t)]^3. \tag{23}$$

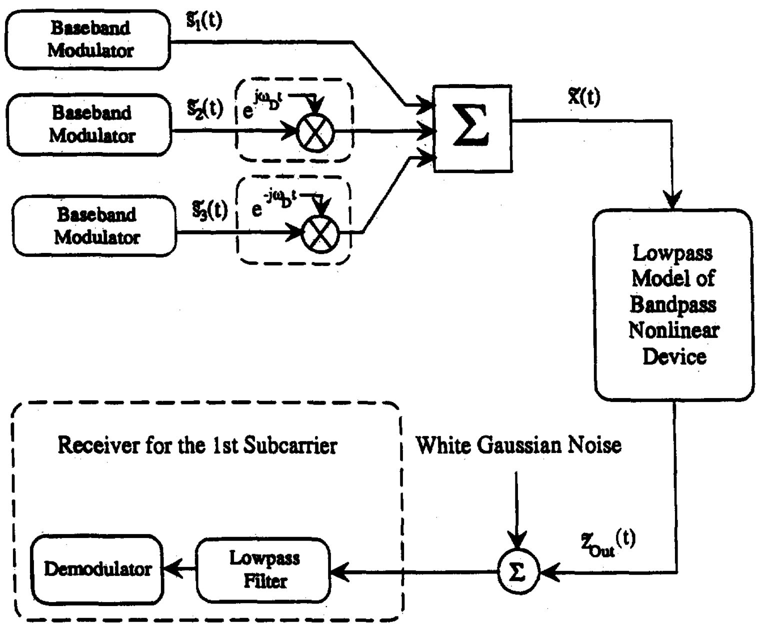

Fig. 4. Block diagram of the communication system model used for the analytic ParSOP method example.

Using (15), the ParSOP method can be applied, and the output signal within the subchannel of interest can be written as

$$\tilde{z}_{\mathrm{Out},\omega_1=0}(t) = C_0\tilde{s}_1(t) + C_1(|\tilde{s}_1(t)|^2\tilde{s}_1(t) + 2|\tilde{s}_3(t)|^2\tilde{s}_1(t) + 2|\tilde{s}_2(t)|^2\tilde{s}_1(t) + \tilde{s}_1^*(t)\tilde{s}_2(t)\tilde{s}_3(t)). \quad (24)$$

Let the modulated subcarriers in the input signal $\tilde{x}(t)$ be of the same modulation type and bit rate. These signals can then be expressed as

$$\tilde{s}_1(t) = \sum_{i=-\infty}^{\infty} a_i p(t - iT + \Delta_1) \quad (25a)$$

$$\tilde{s}_2(t) = \sum_{i=-\infty}^{\infty} b_i p(t - iT + \Delta_2) \quad (25b)$$

$$\tilde{s}_3(t) = \sum_{i=-\infty}^{\infty} c_i p(t - iT + \Delta_3) \quad (25c)$$

where $p(t)$ represents the pulse shaping function and the random sequences $\{a_i\}, \{b_i\}$, and $\{c_1\}$ are obtained from the modulating data. The delays Δ_1, Δ_2, and Δ_3 allow for a variation in the bit timings between the signals. By substituting (25) into (24), we obtain

$$\tilde{z}_{\mathrm{Out},\omega_1=0}(t) = \sum_{l=-\infty}^{\infty} p(t - lT + \Delta_1)][C_0 a_l + C_1 w_l(t)] \quad (26)$$

where

$$w_l(t) = \sum_{i=-\infty}^{\infty}\sum_{j=-\infty}^{\infty} [a_l a_i a_j^* p(t - iT + \Delta_1)p(t - jT + \Delta_1) + 2a_l b_i b_j^* p(t - iT + \Delta_2)p(t - jT + \Delta_2) + 2a_l c_i c_j^* p(t - iT + \Delta_3)p(t - jT + \Delta_3) + 2a_l^* b_i c_j p(t - iT + \Delta_2)p(t - jT + \Delta_3)]. \quad (27)$$

Although more complicated modulation formats can be analyzed, for simplicity we assume binary phase reversal keying (BPRK) with signaling pulses that are a unity amplitude constant amplitude A over a bit period and zero otherwise. In other words, $p(t) = A\Pi(t/T)$, where $\Pi(t/T)$ represents a square pulse centered at zero and having width T. It is also assumed that each modulated subcarrier has the same delay ($\Delta_1 = \Delta_2 = \Delta_3$) which we will set equal to zero without loss of generality.)

The probability of bit error for this system can be easily determined (for an AWGN channel) by using the analytic ParSOP method. We begin by finding $\tilde{z}_{\mathrm{Out},\omega_1=0}(t)$ as defined by (26). Since BPRK modulation is assumed, the variables a_i, b_i, and c_i are real and take on the values of -1 and 1 with equal probability. Because the modulating pulses are nonzero only for a single nonoverlapping bit period, the cross-product terms in $w_l(t)$ are all zero and (26) reduces to

$$\begin{aligned}\tilde{z}_{\mathrm{Out},\omega_1=0}(t) &= \sum_{k=-\infty}^{\infty} \Big[C_0 a_k \Pi(t - kT) + C_1(a_k^3 + 2b_k^2 a_k + 2c_k^2 a_k + 2a_k b_k c_k)A^3\Pi(t - kT)\Big] \\ &= \sum_{k=-\infty}^{\infty} \big[C_0 a_k A\,\Pi(t - kT) + C_1(5a_k + 2a_k b_k c_k)A^3\Pi(t - kT)\big]. \quad (28)\end{aligned}$$

The signal at the output of the integrate and dump receiver, at the dump time, is given by

$$A' = [AC_0 + (5 + 2b_k c_k)A^3 C_1]a_k T. \quad (29)$$

An error is made when the noise at the output of the integrator has a magnitude that exceeds the magnitude of A' and a sign that is opposite to that of A'. For a linear BPRK system, the error probability is given by

$$P_E = \frac{1}{2}\operatorname{erfc}\left(\sqrt{\frac{A^2T}{N_0}}\right). \tag{30}$$

We can use this result to find the error probability for our system by conditioning the error probability on the value of the product $b_k c_k$. Since the product $b_k c_k$ takes on the values of 1 and -1 with equal likelihood for BPRK, the error probability can be found by substituting the magnitude of (29) in place of A in (30), for each value of the product $b_k c_k$. The resulting expression for error probability is

$$P_E = \frac{1}{4}\operatorname{erfc}\left(\sqrt{\frac{(AC_0+7A^3C_1)^2T}{N_0}}\right) + \frac{1}{4}\operatorname{erfc}\left(\sqrt{\frac{(AC_0+3A^3C_1)^2T}{N_0}}\right). \tag{31}$$

To compare this expression for the probability of bit error to a similar expression for some other system, we must make the result a function of the ratio E_B/N_0, where E_B is the average received signal energy for one bit interval. Since the product $b_k c_k$ takes on the values of 1 and -1 with equal likelihood for BPRK, the average received signal energy for one bit interval is

$$\begin{aligned} E_B &= \left[\frac{1}{2}(C_0+7A^2C_1)^2 + \frac{1}{2}(C_0+3A^2C_1)^2\right]A^2T \\ &= (C_0^2 + 10A^2C_0C_1 + 29A^4C_1^2)A^2T. \end{aligned} \tag{32}$$

The probability of bit error is then found by making a substitution in (31) for A^2T in terms of the bit energy. The resulting expression is

$$P_E = \frac{1}{4}\operatorname{erfc}\left(\sqrt{\frac{E_B/N_0(C_0+7A^2C_1)^2}{(C_0^2+10A^2C_0C_1+29A^4C_1)}}\right) + \frac{1}{4}\operatorname{erfc}\left(\sqrt{\frac{E_B/N_0(C_0+3A^2C_1)^2}{(C_0^2+10A^2C_0C_1+29A^4C_1)}}\right) \tag{33}$$

Equation (33) has been evaluated and compared with the result given by a conventional simulation for the case of $A = 0.3, C_0 = 1.77188$, and $C_1 = -0.835248$. The parameter A was selected so that the input envelope would be in the interval [0, 0.9], and C_0 and C_1 were selected to fit data taken from the AM/AM portion of the Saleh model [13] over the interval [0, 1]. The comparison between the results obtained through the analytic ParSOP method and those obtained through conventional simulation is shown in Fig. 5, (conventional simulation results are shown for several values of ω_D) from which it can be seen that the ParSOP results agree very well with the results obtained through conventional simulation. In addition, the results from the ParSOP simulation, which is discussed in the next section, agree with both the analytic ParSOP method results and the conventional simulation results.

V. Use of ParSOP in Simulation

As was previously discussed, the simulation of bandpass systems is carried out through the use of equivalent lowpass models. A basic simulation model can be developed as shown in Fig. 6. In this model, the modulated subcarrier in the channel of interest is assumed to be centered at zero frequency as is customary when using lowpass models. Simulations using this model are referred to as conventional simulations. A simulation model for the ParSOP method is shown in Fig. 7, and is based on (15) with ω_k set equal to zero. Both the conventional simulation and ParSOP method simulation models were used to generate the simulation results that appear later in this section.

Since the purpose of the ParSOP method is to reduce the simulation execution time (run time) by reducing the sampling rate that is necessary to produce accurate results, it is necessary to compare the accuracy of the bit error rate (BER) estimates obtained through the use of ParSOP simulation to those obtained through the use of conventional simulation. Although all simulation techniques involve approximations and some degree of modeling error, the ParSOP method introduces additional error when compared to conventional simulation. This error in the BER estimate occurs for two reasons when using the ParSOP simulation technique. First, the intermodulation products (IMP's) that are not centered on the subcarrier of interest are neglected. In addition, changes in the simulation sampling frequency cause changes in the discrete time model of the system. The error due to the neglected IMP's is the residual error that is incurred through the use of the ParSOP method. This error can be isolated and quantified in simulations by running the ParSOP simulation at the same sampling frequency used by the conventional simulation. The additional error, due to the changes in the system model resulting from reductions in the sampling frequency, can then be identified by reducing the sampling rate of the ParSOP simulations.

Two system configurations were simulated to evaluate the performance of the ParSOP method. Both systems included five subcarriers. The baseband modulators in the models shown in Figs. 6 and 7 were each composed of an ideal BPRK baseband modulator followed by a lowpass filter. The only difference between these two systems was the choice of filters and the channel spacing. In System 1, the filters in the modulators and the receivers were all fifth-order Butterworth lowpass filters with 3-dB bandwidths of 1.5 times the bit rate. The frequency spacing between the subcarriers was 4 times the bit rate for System 1. In System 2, the frequency spacing between subcarriers was 8 times the bit rate, the modulator filters were fourth-order Chebyshev lowpass filters with 3-dB bandwidths of 1.83 times the bit rate and a passband ripples of 0.1 dB, and the lowpass filter in the receiver was a fourth-order Chebyshev with a 3-dB bandwidth of 4.14 times the bit rate and 0.2 dB passband ripple. In both systems, the ideal modulators used an amplitude of 0.2 and the nonlinear characteristic was presented by

$$\boldsymbol{h}[V] = 1.77188V - 0.835248V^3 \tag{34}$$

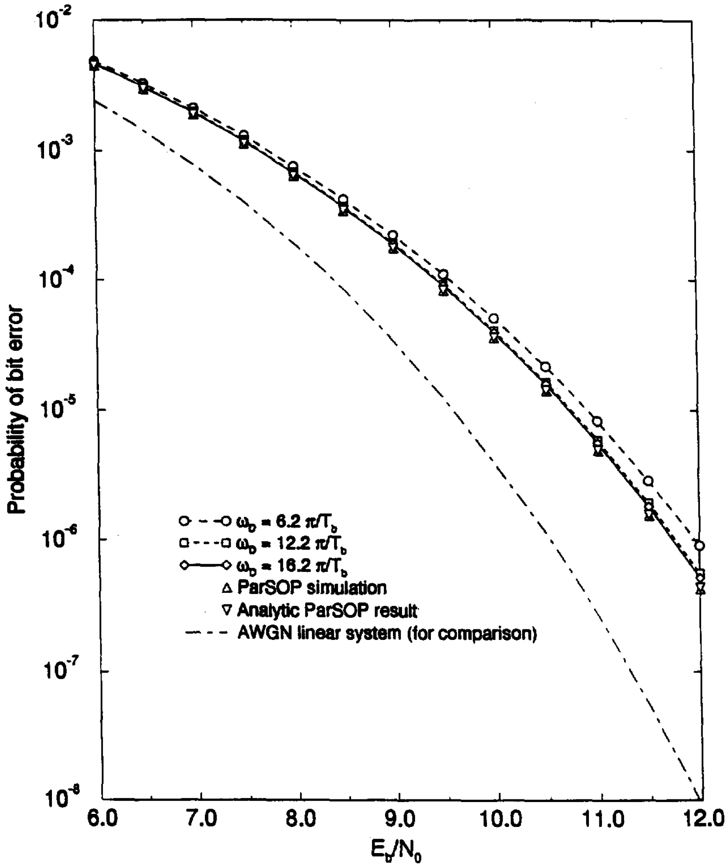

Fig. 5. Simulation and analysis based bit error rate estimates for the system of Fig. 4.

which was obtained by making a minimum mean-square-error fit between the third-order model and 20 sample points obtained from the AM/AM portion of the Saleh model [13] on the interval $0 \leq v \leq 1$, which is the range of the input signal. Although the ParSOP method can be used with any BER estimation technique, semianalytic (sometimes referred to as quasi-analytic) BER estimation [14] was used to produce the results presented here. In these results, the sampling rates and simulation run times have been normalized with respect to the runtime of a conventional simulation operating with a sampling frequency large enough to accurately simulate the system.

Fig. 8 shows the error in the BER estimate (in terms of the E_b/N_0 that was required to product that BER) as a function of the simulation run time for System 1 for three values of the BER. This figure shows that the simulation run time can be reduced by an order of magnitude while only introducing 0.1 dB of error in E_b/N_0. In addition, the error due solely to the neglected IMP's is the error associated with the ParSOP method at a normalized sampling frequency of 1.0. The error component is clearly negligible in the cases presented here. Fig. 9 shows similar results for System 2. In this case, the error is less than 0.04 dB while the sampling frequency is reduced by a factor of 8. In both cases, the ratio of simulation execution times for the ParSOP based simulation and the conventional simulation is very near to the ratio of their respective sampling frequencies.

VI. CONCLUSIONS

In conventional simulation of frequency division multiplexed systems operating over channels containing nonlinear devices, a large sampling frequency must be used to accurately represent the signals involved. The ParSOP method allows the simulation sampling frequency to be reduced by only generating those intermodulation products that are centered in the bandwidth of the single observed modulated subcarrier. Although the direct derivation of the ParSOP method is limited to systems incorporating a complex power series nonlinear model, an alternative derivation allows the use of any memoryless nonlinearity. The results of the alternative derivation might be best applied to systems that contain constant envelope subcarriers, due to the computation burden involved when the modulated subcarriers are not constant envelope signals.

The Analytic ParSOP Method can be used on systems in which an FDM signal is passed through a bandpass nonlinear device. When the spacing between the subcarriers is sufficiently wide to prevent significant overlap in the intermodulation products, the Analytic ParSOP Method will produce excellent results. Conversely, the accuracy of the

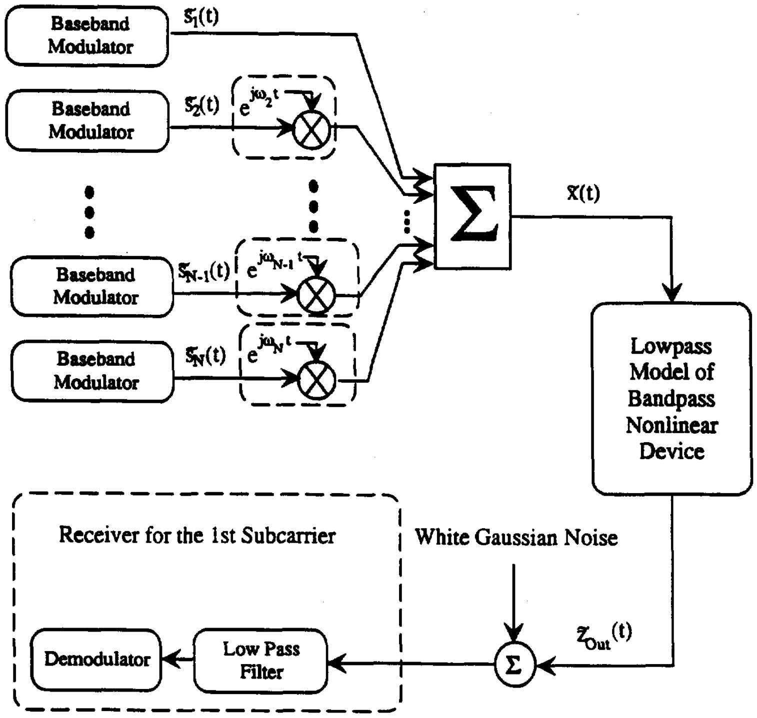

Fig. 6. Block diagram of the conventional simulation model.

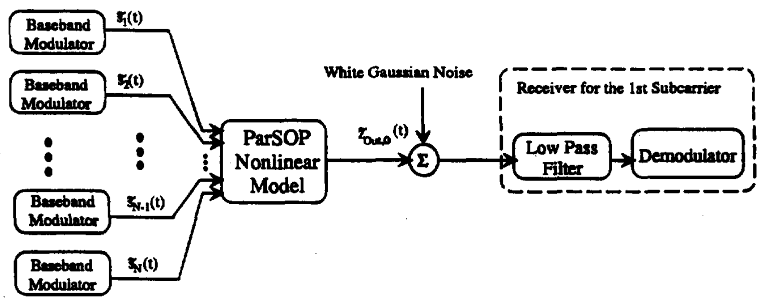

Fig. 7. Block diagram of the ParSOP simulation model.

results produced by this method will be reduced as the spacing between the subcarriers is reduced. Other factors affecting the application of the analytic ParSOP method include the order of the nonlinearity and the number of subcarriers. If either the order of the nonlinearity or the number of carriers is too large, the number of intermodulation products in the subchannel of interest may be so large that an unreasonable amount of effort is required to carry out the analysis. Systems incorporating filters that affect the modulated signals can be analyzed with considerable effort, but the use of a ParSOP simulation of these systems makes much more sense from a practical viewpoint.

Simulation results, obtained by using the complex power series nonlinear model on a filtered BPSK system, showed that a reduction in the simulation run time by an order of magnitude is possible through the use of the ParSOP method on systems involving third-order nonlinearities. In these simulations, the reduction in run time paralleled the reduction in the sampling rate, although an increase in the model order, causing a corresponding increase in the number of intermodulation products, may increase the computational burden of the ParSOP method and cause the reduction in run time to be significantly less than that dictated by a reduction in the sampling frequency.

Appendix
Evaluation of the Shimbo Amplitude Function (SAF)

The Shimbo Amplitude Function (SAF) was introduced in Section III-B as a part of the alternative ParSOP derivation. In this appendix, the SAF is evaluated for several nonlinear models. The SAF is evaluated for several additional nonlinear models in [8] and [15].

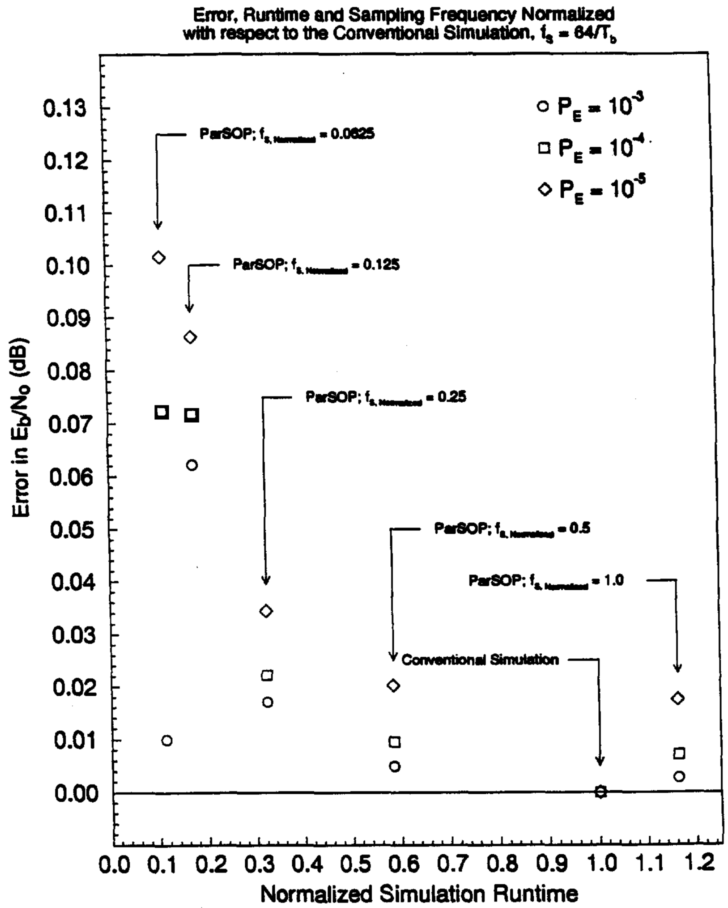

Fig. 8. ParSOP method performance results for System 1.

A. Evaluation of the Shimbo Amplitude Function for the PowerSeries Nonlinear Model

When the nonlinear device characteristic is given by (8), the SAF is given by

$$M(k_1, k_2, \cdots, k_N; t) = \sum_{r=0}^{R} C_r (r+1)! 2^{r+1} \cdot \left\{ \left(-\frac{1}{Y} \cdot \frac{\partial}{\partial Y} \right)^r \frac{\left[\prod_{i=1}^{N} J_{k_i}(V_i(t) Y) \right]}{Y} \right\}_{Y=0}. \quad (35)$$

This expression is obtained through the use of [4]

$$\int_0^\infty G(r)\, dr \int_0^\infty \rho^{2(m+1)} J_1(r\rho)\, d\rho = (m+1)!\, 2^{m+1} \left[\left(-\frac{1}{Y} \frac{\partial}{\partial Y} \right)^m \frac{G(Y)}{Y^2} \right]_{Y=0}. \quad (36)$$

With the inclusion of the partial derivatives, (35) is not particularly suited for numerical evaluation or for use in a simulation. However, it does provide a way to verify the results of the direct derivation of the ParSOP method. This verification is too lengthy to be included here, but it has been carried out for the case of a third-order nonlinearity [8].

B. Evaluation of the SAF for the Bessel Series NonlinearModel

Fuenzalida *et al.* [12] utilized a Bessel function series of the form

$$h[V(t)] = \sum_{r=1}^{R} b_r J_1[\alpha r V(t)] \quad (37)$$

to characterize the memoryless nonlinearity. The Bessel series model is nice because it leads to a simple result for the SAF. In addition, the Bessel series model of the envelope characteristic corresponds to a Fourier series expansion of the instantaneous voltage transfer function. The expression for the SAF is derived in [12] and is given by

$$M(k_1, k_2, \cdots, k_N; t) = \sum_{r=1}^{R} b_r \prod_{i=1}^{N} J_{k_i}[\alpha r V_i(t)]. \quad (38)$$

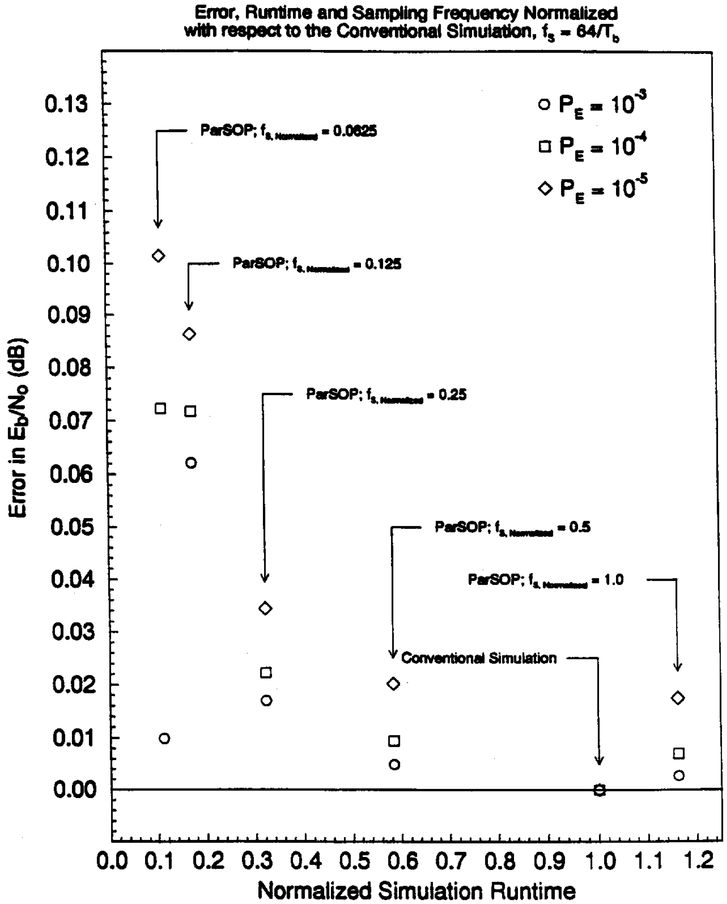

Fig. 9. ParSOP method performance results for System 2.

If the subcarriers have constant envelopes, this formula only need be evaluated once for each set of k_i in a particular system configuration. However, in the general case, it must be evaluated at every step in the simulation. In order to reduce the number of times this formula must be evaluated, the values of k_i can be restricted by only generating the third-order and maybe the fifth-order terms. The order of the term is given by

$$\text{order } = \sum_{i=1}^{N} |k_i|. \tag{39}$$

Since there are only a few third- and fifth-order terms that fall in the bandwidth of interest, this produce can significantly reduce the computational burden involved in implementing this ParSOP model.

References

[1] *IEEE J. Select. Areas Commun.*, vol. SAC-2, Jan. 1984.
[2] *IEEE J. Select. Areas Commun.*, vol. SAC-6, Jan. 1988.
[3] G. J. Foshini and A. A. M. Saleh, "Overcoming optical amplifier intermodulation distortion using coding in multichannel communications systems," *IEEE Trans. Commun.*, vol. COM-38, pp. 187–191, Feb. 1990.
[4] O. Shimbo, "Effects of intermodulation, AM–PM conversion, and additive noise in multicarrier TWT systems," *Proc. IEEE*, vol. 59, pp. 230–238, Feb. 1971.
[5] R. F. Pawula, T. S. Fong, and M. R. O'Sullivan, "Intermodulation distortion in frequency multiplexed satellite repeaters," *Proc. IEEE*, vol. 59, pp. 213–218, Feb. 1971.
[6] R. F. Baum, "The correlation function of smoothly limited Gaussian noise," *IRE Trans. Inform. Theory*, IT-3, pp. 193–197, Sept. 1957.
[7] R. G. Lyons, "A stochastic analysis of signal sharing in a bandpass nonlinearity," *IEEE Trans. Commun.*, vol. COM-22, pp. 1778–1788, Nov. 1974.
[8] K. W. Schneider, "Modeling of intermodulation products for efficient simulation of multi-carrier digital communication systems," Ph.D. dissertation, Univ. Missouri–Rolla, 1992.
[9] W. B. Davenport, Jr., and W. L. Root, *An Introduction to the Theory of Random Signals and Noise*. New York: IEEE Press, 1987, p. 287.
[10] D. D. Siljak, *Nonlinear Systems*. New York: Wiley, 1969.
[11] R. Blum and M. C. Jeruchim, "Modeling nonlinear amplifiers for communication simulation," in *ICC Conf. Proc.*, 1989, pp. 1468–1472.
[12] J. C. Fuenzalida, O. Shimbo, and W. L. Cook, "Time-domain analysis of intermodulation effects caused by nonlinear amplifiers," *COMSAT Tech. Rev.*, vol. 3, no. 1, pp. 89–143, Spring 1973.
[13] A. A. M. Saleh, "Frequency-independent and frequency-dependent nonlinear models of TWT amplifiers," *IEEE Trans. Commun.*, vol. COM-29, Nov. 1981.
[14] M. C. Jeruchim, P. Balaban, and K. S. Shanmugan, *Simulation of Communication Systems*. New York: Plenum, 1992.
[15] A. A. M. Saleh, "Intermodulation analysis of FDMA satellite systems employing compensated and uncompensated TWT's," *IEEE Trans. Commun.*, vol. COM-30, pp. 1233–1242, May 1982.

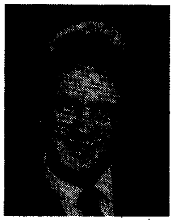

Kevin W. Schneider (S'83–M'92) was born in Maryville, MO, in 1963. He received the B.S. (summa cum laude), M.S., and Ph.D. degrees in electrical engineering from the University of Missouri–Rolla in 1986, 1989, and 1992, respectively.

He worked the summer of 1987 at the Naval Research Laboratory in Washington, DC, and the summer of 1988 at the Naval Underwater Systems Center in New London, CT. He is presently employed as a Staff Scientist at ADTRAN in Huntsville, AL, where he is involved with the development of signal processing algorithms for use in digital telecommunication equipment.

Dr. Schneider is a member of the IEEE Communications Society, the IEEE Education Society, and the American Society for Engineering Education. He was awarded the Office of Naval Research Graduate Fellowship in 1986.

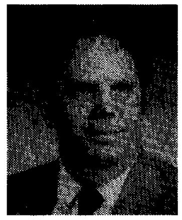

William H. Tranter (S'63–M'68–SM'80–F'85) received the B.S.E.E., M.S.E.E., and Ph.D. degrees from the University of Alabama, Tuscaloosa, in 1964, 1965, and 1970, respectively.

In September 1969 he joined the Faculty of the University of Missouri–Rolla and was named Professor of Electrical Engineering in 1975. His duties in the Department of Electrical Engineering involve the direction of research as well as teaching undergraduate and graduate courses in communications and signal processing. His research interests lie in the areas of digital signal processing and computer-aided design and analysis of communication systems. His research efforts have been supported by the National Aeronautics and Space Administration, GE Aerospace, and the National Science Foundation. His consulting activities have involved the Education Development Corporation, Battelle Memorial Institute, Motorola Incorporated, and the McDonnell Douglas Corporation. He is the author of numerous technical papers and is coauthor of two textbooks entitled *Principles of Communications: Systems Modulation and Noise* (Boston, MA: Houghton-Mifflin, 1976, 1984, 1990), and *Signals and Systems: Continuous and Discrete* (New York: Macmillan, 1983, 1989, 1993). From 1980 to 1985 he served as Assistant and Associate Dean of Engineering for Research and Graduate Affairs at the University of Missouri–Rolla. In 1985 he was named Schlumberger Professor of Electrical Engineering and continues to serve in that position.

Dr. Tranter is a member of Sigma Xi, Eta Kappa Nu, Phi Kappa Phi, Tau Beta Pi, and the American Society for Engineering Education. Within the IEEE Communications Society, he has served as the Chairman of both the Data Communication Sytems Committee and the Educational Services Committee. He has served on the Advisory Board, Advisor to the Communications Society Conference Board, the Awards Board and in the Department of Meetings and Conferences. He currently serves as Editor-in-Chief of the IEEE JOURNAL ON SELECTED AREAS IN COMMUNICATIONS. In 1989 he received the Donald W. McLellan Meritorious Service Award from the IEEE Communications Society.